Oxygen and water-related impurities in C_{60} crystals: A density-functional theory study

L. Tsetseris[1,2] and S. T. Pantelides[2,3]
[1]*Department of Physics, National Technical University of Athens, GR-15780 Athens, Greece*
[2]*Department of Physics and Astronomy, Vanderbilt University, Nashville, Tennessee 37235, USA*
[3]*Oak Ridge National Laboratory, Oak Ridge, Tennessee 37831, USA*
(Received 18 May 2010; revised manuscript received 16 June 2010; published 6 July 2010)

Despite the importance of impurity effects for the use of the prototype organic semiconductor C_{60} in modern electronics, the atomic-scale mechanisms which underlie several key oxygen-induced modifications of C_{60} crystal properties remain elusive. Here we use first-principles calculations to address varying, and, in cases, seemingly conflicting experimental data on oxygen or water incorporation in crystalline C_{60}. We clarify the role of several oxygen- and water-related configurations, including spin-polarized physisorbed structures, chemisorbed geometries, and polymer precursors, in the creation of deep traps, shallow traps, or resonances. The role of annealing is thus clarified in producing a hierarchy of impurity-related effects in C_{60}.

DOI: 10.1103/PhysRevB.82.045201 PACS number(s): 72.80.Le, 71.20.Rv, 71.55.Ht

I. INTRODUCTION

The molecular crystals of the carbon allotrope fullerene C_{60}, also known as fullerites, have been recognized over the years as a prototype environment to probe fundamental mechanisms of transport and optoelectronic processes. Moreover, relatively high carrier mobilities and high electron affinity make fullerites the materials of choice for applications in electronic devices, such as field-effect transistors[1] or photovoltaics.[2] However, the physical properties of organic semiconductors in general, and fullerites in particular, are often susceptible to significant modification due to insertion of extrinsic species.[3] Numerous experiments have long reported[4–16] evidence for the sensitivity of fullerites to incorporation of impurities, such as oxygen and water.

Oxygen may be absorbed in C_{60} crystals either in molecular form, or, following annealing at elevated temperatures, in chemisorbed configurations of atomic O. Oxygen insertion is accompanied with decrease of conductivity, which in certain cases, and similar to other organic semiconductors,[17–20] relates to the appearance of levels[4,7,9–11,13,14,16,21] in the energy band gap of fullerites. Computational studies[22–24] have probed the stability of chemisorbed O impurities on individual fullerene molecules. A resolution of the origins of impurity-related degradation, however, can be attained only with pertinent studies on C_{60} crystals, wherein there are enhanced possibilities of adsorption and, concomitantly, of more complex impurity effects.

In this paper we probe with extensive first-principles calculations oxygen- and water-related effects on individual C_{60} molecules, but also in crystalline C_{60} supercells. We outline the sequence of reactions that may lead from physisorbed O_2 molecules to chemisorbed O atoms on fullerenes under annealing. Both nondissociated oxygen molecules in C_{60} crystalline voids and certain chemisorbed structures generate levels in the energy band gap of C_{60}, creating thus shallow and deep energy traps for charge carriers. In contrast, water molecules have minimal effect on the electronic properties of C_{60} crystals, unless conditions favor hydrolysis and formation of isolated hydroxyl groups on fullerene molecules.

II. METHOD

The results were obtained using the density-functional theory (DFT) code VASP (Ref. 25) with ultrasoft pseudopotentials[26] and a local-density approximation[27] (LDA) exchange-correlation (xc) functional. Selected calculations were also performed with a generalized-gradient approximation (GGA) xc-functional.[28] Unless stated otherwise, the results we present below are LDA values. The cutoff for the plane wave basis was set to 300 eV. Calculations for impurities in crystals employed supercells with 4 C_{60} molecules in a face-centered cubic (FCC) arrangement and $3\times3\times3$ k grids.[29] Electronic densities of states (DOS) were obtained with k-sampling through the tetrahedron method.[30] Barriers were obtained with the nudged elastic band (NEB) method,[31] based on experience with calculations of activation energies in various systems.[32,33]

The selection of an LDA functional, instead of a GGA approach, relates to how these two classes of DFT functionals perform in the case of graphitic systems. In particular, it is known that while GGA calculations fail to account for any binding between graphite layers,[34,35] LDA studies obtain graphite interlayer distances and binding energies which are in satisfactory agreement with experimental values, even though van der Waals interactions are not included explicitly. The relatively satisfactory LDA description of the energetics and electronic properties of carbon-based systems extends also to fullerites and carbon nanotubes.[34] Methods, such as the GW scheme,[36] that go beyond the LDA and yield energy band gaps in better agreement with experimental values are not employed here because at present they require excessive computational power, especially in the case of large defect supercells.

III. RESULTS AND DISCUSSION

An understanding of the stability of oxygen impurities in fullerites presupposes knowledge of equilibrium structures of oxygen species on isolated C_{60} molecules. The most stable configurations of atomic O on a fullerene molecule are shown in Fig. 1. In agreement with previous studies,[22,23] the

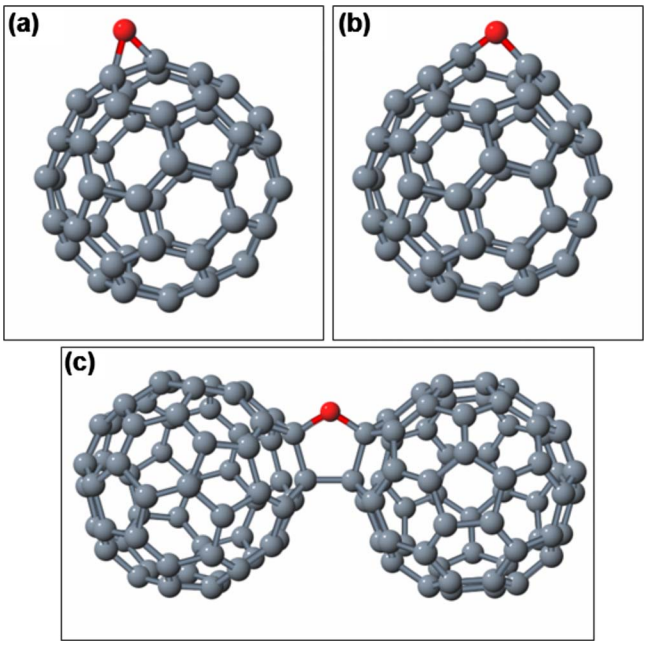

FIG. 1. (Color online) Oxygen impurities on a C_{60} molecule: O bridges (a) on a (6,6) bond and (b) a (6,5) bond. (c) O bridge between two C_{60} molecules. [Carbon: gray, Oxygen: dark gray (red) spheres]

lowest energy structures correspond to O bridges above (6,6) and (6,5) C_{60} bonds. Within LDA (GGA) the (6,5) structure is only 0.03 eV (0.02 eV) lower than the (6,6) configuration. Other metastable O geometries are the endohedral configuration with O at the center of the fullerene, and O chemisorbed in bridge configuration inside the C_{60} cage. The energies of these structures are 4.42 and 3.11 eV, respectively, higher than that of the (6,5) bond.

The adsorption of molecular oxygen can lead to several different types of configurations. First, as shown in Fig. 2(a), the molecule can physisorb above a (6,6) bond with a binding energy of 0.5 eV. The molecule can then get attached[24] to the fullerene in the form of Fig. 2(b). The energy gain and barrier of this process are 0.75 and 0.67 eV, respectively. Subsequently, the attached molecule can dissociate to a pair of carbonyl groups or a pair of vicinal (6,5) O bridges. The energies of these structures, which are depicted in Figs. 2(c) and 2(d), are lower than that of Fig. 2(b) by 0.93 and 2.30 eV, respectively. A similar sequence of transformations takes place over defects of graphene and carbon nanotubes.[37] The activation energies for the (b) to (c) and (b) to (d) transformations are 1.45 and 1.40 eV. Overall, the reaction energies and barriers indicate, in agreement with experiments,[38,39] that increasing the annealing temperature during exposure of C_{60} to molecular oxygen can enable first the adsorption of nondissociated O_2 species, followed by the dissociation to very stable chemisorbed pairs of vicinal O atoms.

Atomic O impurities in crystalline C_{60} can reside on one fullerene molecule, or serve as bridges between two neighboring molecules.[40–43] In fact, O-related bonds can serve as anchors between other graphitic systems, such as carbon nanotubes,[44] and the surrounding chemical environment. The most stable O configuration in C_{60} fullerite is the intermo-

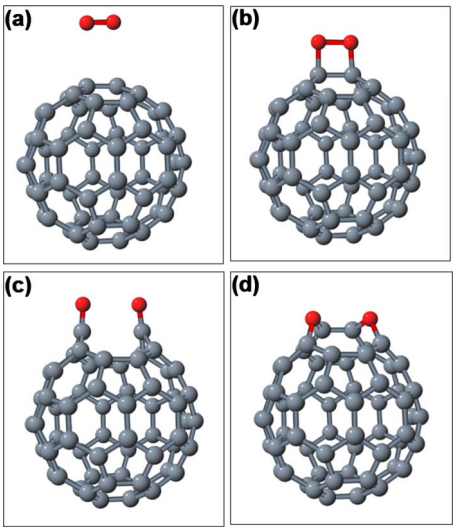

FIG. 2. (Color online) Adsorption of an oxygen molecule on a C_{60} molecule: (a) physisorbed and (b) chemisorbed O_2 molecule, (c) pairs of vicinal carbonyl groups, (d) pairs of vicinal (6,5) O bridges. [Carbon: gray, oxygen: dark gray (red) spheres]

lecular bridge (IB) of the type of Fig. 1(c). Compared to this structure, the energy increases by 0.6 eV when the O bridge is replaced by a C-C intermolecular bridge and the O impurity moves to a vicinal (6,5) position on one of the moieties of the C_{60} dimer. Other structures with nondimerized molecules and an O atom on an individual C_{60} have energies higher than that of IB by 1.0–1.1 eV. An intermolecular C-O-C bridge configuration with no direct intermolecular C-C bonds is less stable than IB by 1.6 eV.

Figure 3 depicts the electronic densities of states (DOS) for pristine C_{60} crystals and for fullerites with an O impurity of the type of Fig. 1(c). The calculated energy band gap (1.07 eV) is significantly less than the experimental value (which is more than[4] 2.1 eV), a well-known limitation of DFT approaches. With respect to impurity-related effects we note that the IB of Fig. 1(c) creates resonancelike DOS peaks at

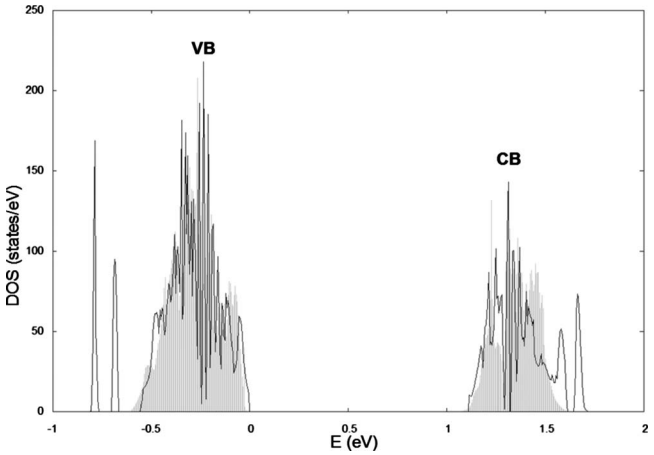

FIG. 3. Electronic densities of states (DOS) for pristine C_{60} crystal (shaded), and for crystalline C_{60} with O impurities of the type of Fig. 1(c) (solid line). Zero of energy is set at the valence band (VB) maximum.

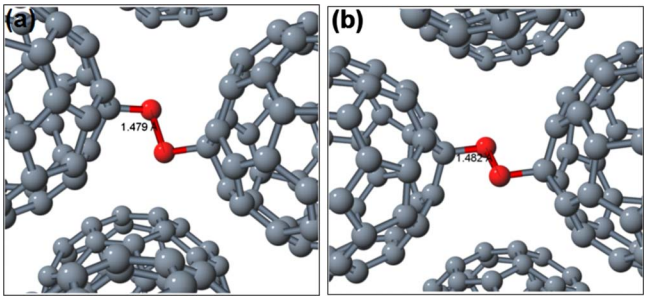

FIG. 4. (Color online) Formation of intermolecular O_2 bridges in a C_{60} crystal. The energies of configurations (a) and (b) are approximately the same as those of O_2 molecules in octahedral and tetrahedral voids, respectively. [Carbon: gray, oxygen: dark gray (red) spheres]

the top of the valence band, as well as states between the highest-occupied molecular orbital (HOMO) and HOMO-1 bands. DOS results for O bridges on individual C_{60} molecules have minimal differences with respect to the DOS of pristine fullerite. Overall, the presence of exohedral atomic O impurities, either in the core of C_{60} dimers, or on individual C_{60} molecules does not create defect levels in the energy band gap of the host fullerene crystal.

As noted above, the energies of configurations with an oxygen atom inside the C_{60} cage are significantly higher (by more than 3.11 eV) than those of structures of Figs. 1(a) and 1(b). Nevertheless, O atoms that are trapped inside a fullerene molecule during synthesis or other special conditions, such as irradiation, can remain in endohedral configurations for a prolonged period of time due to high energy barriers of escape. Indeed, the calculated activation energy for transformation of endo- to exohedral O configuration is so high (about 3.0 eV) that the process is not operative at room or moderate temperatures. The presence of these trapped oxygen species introduces distinct peaks in the fullerite DOS, with the most important feature the appearance of shallow traps about 0.05 eV above the valence band maximum.

When oxygen enters a C_{60} crystal in molecular form it can occupy the center of crystalline voids. In agreement with suggestions from experimental data,[12,45] we found that the octahedral voids are more efficient (by 0.23 eV) O_2 trapping sites than the tetrahedral positions. In both octahedral and tetrahedral lowest-energy configurations, the O_2 molecule retains its gas-phase $2\mu_B$ magnetic moment and is aligned along the crystalline (111) direction. Other stable nondissociated O_2 structures are shown in Fig. 4. These intermolecular bridges are formed in the tight space between neighboring C_{60} molecules. The bridges of Figs. 4(a) and 4(b), which have O-O bonds stretched to 1.48 Å, are comparable in energy to octahedral and tetrahedral structures, respectively.

Annealing of a C_{60} crystal with O_2 molecules can enable first the attachment of the impurity molecule to fullerene species, or even the complete dissociation and chemisorption in the form of atomic O. In particular, an impurity configuration of the type of Fig. 2(b) is more stable than octahedral O_2 structures by 0.65 eV. Heating at higher temperatures can lead to dissociation of the O_2 entity and creation of atomic O

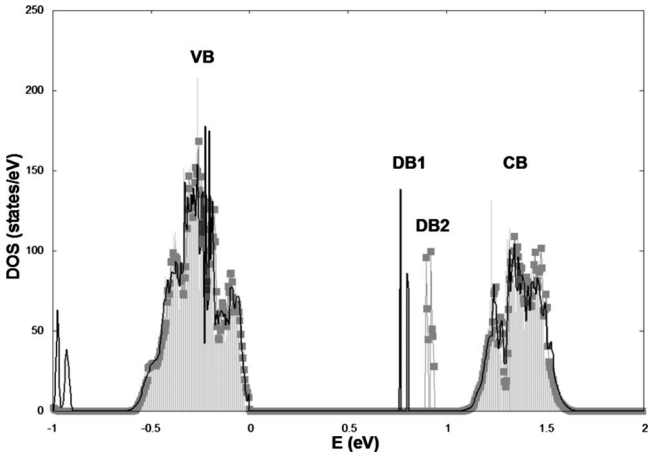

FIG. 5. Electronic densities of states (DOS) for pristine C_{60} crystal (shaded), and for crystalline C_{60} with O_2 molecules in the tetrahedral (solid line) and octahedral (line with squares) voids. Zero of energy is set at the valence band (VB) maximum. The impurities introduce pairs of defect levels (DB1 and DB2) in the C_{60} energy band gap.

bridges. These processes lead to significant drops of 2.5–3.0 eV in energy when compared to octahedral trapping.

As shown in the DOS plots of Fig. 5, O_2 molecules trapped at octahedral or tetrahedral C_{60} voids introduce pairs of defect levels in the fullerite energy band gap. These levels lie deep inside the band gap and can act as efficient traps of charge carriers. Deep traps are created also when O_2 species form bridges of the type of Fig. 4. When the O_2 molecule reacts with C_{60} to form impurities of the type of Figs. 2(b) and 2(d) the traps disappear, but new features emerge in the DOS plots. Specifically, resonancelike peaks (denoted R1 and R2 in Fig. 6) appear at the valence band maximum and conduction band minimum, suggesting an important role of

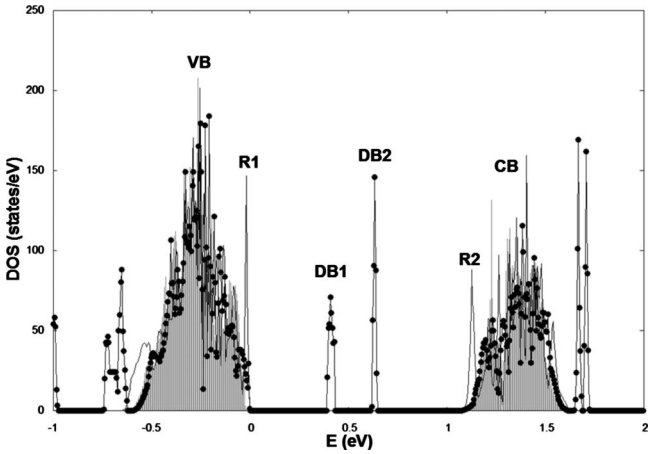

FIG. 6. Electronic densities of states (DOS) for pristine C_{60} crystal (shaded), for crystalline C_{60} with O_2 molecules in the impurity configuration of Fig. 4(b) (line with squares), and for a C_{60} crystal with a defective molecule of the type shown in Fig. 2(d) (solid line). Zero of energy is set at the valence band (VB) maximum. The impurities introduce pairs of defect levels (DB1 and DB2) in the C_{60} energy band gap, or resonances (R1 and R2) at the VB maximum and conduction band (CB) minimum.

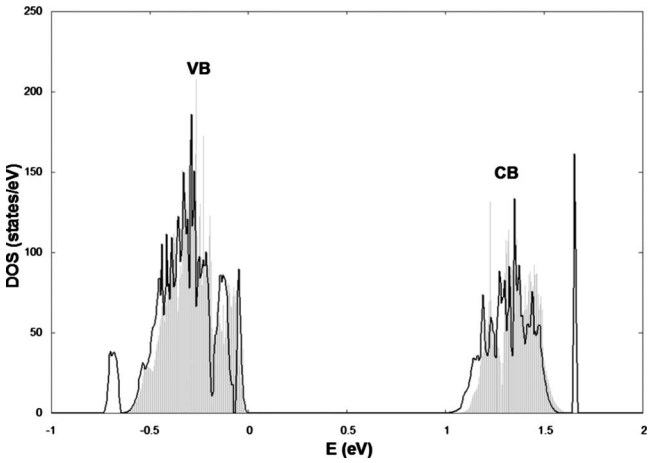

FIG. 7. Electronic densities of states (DOS) for crystalline C_{60} with no impurities (shaded) and with vicinal H and OH impurities on a C_{60} molecule (solid line). Zero of energy is set at the valence band (VB) maximum.

chemisorbed O impurities in carrier scattering and, concomitantly, mobility degradation of the host crystal.

Similar to oxygen, H_2O molecules can be absorbed intact in the octahedral or tetrahedral voids of C_{60} crystals, with the former being more favorable energetically by 0.1 eV. When they retain a molecular form, water-related impurities introduce only very small changes in the DOS plot of crystalline C_{60}. In contrast, a pair of vicinal H and OH impurities attached on nearest C atoms of a C_{60} molecule creates a discrete peak at the top of the valence band. The corresponding DOS results are shown in Fig. 7. The most stable structure for the H-OH pair is the one with the corresponding C atoms across a (6,6) bond. The energy of this configuration is about 0.1 eV lower than that of an H_2O molecule in an octahedral void. Though first-principles calculations for lower concentrations of impurities are presently impractical, the results of Fig. 7 suggest that at the dilute limit the H-OH impurities may introduce a shallow hole trap in fullerites.

As noted above, experimental reports about the effect of O_2 and H_2O impurities on the electronic spectrum of C_{60} are varying. Specifically, some experiments have linked the presence of oxygen impurities to deep traps[7,9–11] in the fullerite energy band gap, while other works have found that shallow traps[4,21] are formed under exposure to air. In addition, there are also reports[8] which proposed that exposure to oxygen creates no levels in the fullerite band gap. The results of this work elucidate the atomic-scale details behind these varying observations by identifying several different oxygen-related configurations which can indeed account for formation of deep traps, shallow traps, or no traps. Likewise, the results described above are consistent with observations[15] of a minimal effect of intact water impurities, but also identify hydrolysis as a process that may lead to resonances or shallow traps in fullerites.

In summary, we have the described the energetics of oxygen adsorption on C_{60} molecules and the atomic-scale details of oxygen and water insertion in C_{60} crystals. The impurities give rise to various distinct configurations which can account for experimental observations of creation of carrier traps, deep or shallow, in C_{60} fullerite.

ACKNOWLEDGMENTS

This work was supported in part by the William A. and Nancy F. McMinn Endowment at Vanderbilt University, by DOE Grant No. DEFG0203ER46096, and by DTRA Grant No. HDTRA 1-10-1-0016. The calculations were performed at ORNL's Center for Computational Sciences.

[1] A. R. Murphy and J. M. J. Fréchet, Chem. Rev. **107**, 1066 (2007).
[2] Y. Shirota and H. Kageyama, Chem. Rev. **107**, 953 (2007).
[3] H. Sirringhaus, Adv. Mater. **21**, 3859 (2009).
[4] T. Arai, Y. Murakami, H. Suematsu, K. Kikuchi, Y. Achiba, and I. Ikemoto, Solid State Commun. **84**, 827 (1992).
[5] Z. Belahmer, P. Bernier, L. Firlej, J. M. Lambert, and M. Ribet, Phys. Rev. B **47**, 15980 (1993).
[6] A. Zahab and L. Firlej, Solid State Commun. **87**, 893 (1993).
[7] S. Fujimori, K. Hoshimono, S. Fujita, and S. Fujita, Solid State Commun. **89**, 437 (1994).
[8] S. Kazaoui, R. Ross, and N. Minami, Solid State Commun. **90**, 623 (1994).
[9] C. H. Lee, G. Yu, B. Kraabel, D. Moses, and V. I. Srdanov, Phys. Rev. B **49**, 10572 (1994).
[10] V. I. Srdanov, C. H. Lee, and N. S. Sariciftci, Thin Solid Films **257**, 233 (1995).
[11] E. A. Katz, V. Lyubin, D. Faiman, S. Shtutina, A. Shames, and S. Goren, Solid State Commun. **100**, 781 (1996).
[12] B. Pevzner, A. F. Hebard, and M. S. Dresselhaus, Phys. Rev. B **55**, 16439 (1997).
[13] A. Tapponnier, I. Biaggio, and P. Günter, Appl. Phys. Lett. **86**, 112114 (2005).
[14] M. Rusu, J. Strotmann, M. Vogel, M. C. Lux-Steiner, and K. Fostiropoulos, Appl. Phys. Lett. **90**, 153511 (2007).
[15] A. P. Saab, M. Laub, V. I. Srdanov, and G. D. Stucky, Adv. Mater. **10**, 462 (1998).
[16] H. Habuchi, S. Nitta, D. Han, and S. Nonomura, J. Appl. Phys. **87**, 8580 (2000).
[17] L. Tsetseris and S. T. Pantelides, Phys. Rev. B **75**, 153202 (2007).
[18] L. Tsetseris and S. T. Pantelides, Phys. Rev. B **78**, 115205 (2008).
[19] L. Tsetseris and S. T. Pantelides, Org. Electron. **10**, 333 (2009).
[20] L. Tsetseris and S. T. Pantelides, Eur. Phys. J.: Appl. Phys. **46**, 12511 (2009).
[21] T. Matsushima, M. Yahiro, and C. Adachi, Appl. Phys. Lett. **91**, 103505 (2007).
[22] M. Menon and K. R. Subbaswamy, Phys. Rev. Lett. **67**, 3487 (1991).
[23] K. Raghavachari, Chem. Phys. Lett. **195**, 221 (1992).
[24] Z. Shang, Y. Pan, H. Wang, Z.-S. Cai, X. Z. Zhao, J. Feng, and

A. Tang, J. Mol. Struct.: THEOCHEM **392**, 217 (1997).
[25] G. Kresse and J. Furthmuller, Phys. Rev. B **54**, 11169 (1996).
[26] D. Vanderbilt, Phys. Rev. B **41**, 7892 (1990).
[27] J. P. Perdew and A. Zunger, Phys. Rev. B **23**, 5048 (1981).
[28] J. P. Perdew and Y. Wang, Phys. Rev. B **45**, 13244 (1992).
[29] D. J. Chadi and M. L. Cohen, Phys. Rev. B **8**, 5747 (1973).
[30] O. Jepson and O. K. Andersen, Solid State Commun. **9**, 1763 (1971).
[31] G. Mills, H. Jónsson, and G. K. Schenter, Surf. Sci. **324**, 305 (1995).
[32] L. Tsetseris and S. T. Pantelides, Phys. Rev. Lett. **97**, 116101 (2006); L. Tsetseris, X. J. Zhou, D. M. Fleetwood, R. D. Schrimpf, and S. T. Pantelides, IEEE Trans. Device Mater. Reliab. **7**, 502 (2007).
[33] L. Tsetseris, N. Kalfagiannis, S. Logothetidis, and S. T. Pantelides, Phys. Rev. Lett. **99**, 125503 (2007); L. Tsetseris and S. T. Pantelides, Acta Mater. **56**, 2864 (2008).
[34] L. A. Girifalco and M. Hodak, Phys. Rev. B **65**, 125404 (2002).
[35] N. Ooi, A. Rairkar, and J. B. Adams, Carbon **44**, 231 (2006).
[36] M. L. Tiago, J. E. Northrup, and S. G. Louie, Phys. Rev. B **67**, 115212 (2003).
[37] L. Tsetseris and S. T. Pantelides, J. Phys. Chem. B **113**, 941 (2009).
[38] H. S. Chen, A. R. Kortan, R. C. Haddon, M. L. Kaplan, C. H. Chen, A. M. Mujsce, H. Chou, and D. A. Fleming, Appl. Phys. Lett. **59**, 2956 (1991).
[39] G. H. Kroll, P. J. Benning, Y. Chen, T. R. Ohno, J. H. Weaver, L. P. F. Chibante, and R. E. Smalley, Chem. Phys. Lett. **181**, 112 (1991).
[40] L. Dunsch, P. Rapta, A. Gromov, and A. Stasko, J. Electroanal. Chem. **547**, 35 (2003).
[41] J. Zhang, K. Porfyrakis, M. R. Sambrook, A. Ardavan, and G. A. D. Briggs, J. Phys. Chem. B **110**, 16979 (2006).
[42] P. Paul, K. C. Kim, D. Sun, P. D. W. Boyd, and C. A. Reed, J. Am. Chem. Soc. **124**, 4394 (2002).
[43] F. J. Owens, Z. Iqbal, L. Belova, and K. V. Rao, Phys. Rev. B **69**, 033403 (2004).
[44] L. Tsetseris and S. T. Pantelides, Phys. Rev. Lett. **97**, 266805 (2006).
[45] B. Renker, H. Schober, M. T. Fernandez-Diaz, and R. Heid, Phys. Rev. B **61**, 13960 (2000).